



A Systematic Approach to Chest Radiographic Analysis

1

Jeffrey S. Klein and Melissa L. Rosado-de-Christenson

Learning Objectives

- List the nine components of a chest radiographic examination to be systematically analyzed.
- Identify key technical quality aspects to be assessed prior to interpretation of a chest radiograph.
- Identify the normal anatomic structures and interfaces routinely displayed on chest radiographic examinations.
- Detail the different patterns of lung disease seen radiographically.
- Describe the different appearances of pleural disease seen on chest radiography.

1.1 Introduction

The chest radiograph remains one of the most commonly performed examinations in radiology. It is typically the first radiologic examination obtained in patients presenting with chest pain, shortness of breath, or cough. In the hospital setting, chest radiographs are performed in the emergency room, critical care unit, and following the placement of monitoring and support devices. Chest radiographs are routinely obtained prior to major surgical procedures, as part

J. S. Klein (✉)
Department of Radiology, University of Vermont College of Medicine, Burlington, VT, USA
e-mail: jsklein@uvm.edu

M. L. Rosado-de-Christenson
Department of Radiology, Saint Luke's Hospital of Kansas City, Kansas City, MO, USA

Department of Radiology, University of Missouri-Kansas City, Kansas City, MO, USA
e-mail: mrosado@saint-lukes.org

of annual physical examinations, and to screen for metastatic disease in patients with malignancy or paraneoplastic syndromes.

The accurate interpretation of chest radiographs requires an understanding of the normal frontal and lateral chest radiographic appearances, as obscuration of normally visualized structures may be the only clue to the presence of an abnormality.

Radiography allows visualization and assessment of the chest wall, mediastinum, and hila including the heart and great vessels, central airways, the lungs including the pulmonary vasculature, the pleural surfaces including the fissures and the diaphragm.

The superimposition of complex structures of various radiographic density (gas, water, calcium, metal, and fat) makes radiographic interpretation challenging. An understanding of normal interfaces allows for detection of conditions that manifest with chest symptoms or as asymptomatic abnormalities.

1.2 A Systematic Assessment

We present a systematic approach to the analysis of chest radiographs (Table 1.1). This should begin with an assessment of technical aspects of the radiographic study including patient positioning, mediastinal penetration, sharpness of structures (to detect motion), lung volumes, and presence of artifacts [1] to allow for accurate detection of abnormalities. The orderly assessment of each anatomic region and structure will yield a comprehensive imaging evaluation, will allow identification of subtle abnormalities, and will minimize interpretive errors. The following must be evaluated in each chest radiograph: support and monitoring devices (if present), chest wall, heart and mediastinum, hila, lungs, airways, pleura, and diaphragm.

Table 1.1 Systematic analysis of chest radiographs

Component evaluated	Assessment
Technical quality	Positioning, penetration, motion, lung volumes, artifacts
Support/monitoring devices	ET/NG tube, vascular catheters, pacemaker
Chest wall	Absence of normal contour, swelling, mass, calcification, air, osseous abnormality
Mediastinum	Cardiomegaly, mass, widening, position, calcification, air
Hila	Height (right vs left), size, density, contour
Lungs	Atelectasis Air space opacities Interstitial lung disease Focal opacities (solitary pulmonary nodules/masses Abnormal lucency-localized/unilateral/diffuse
Airways	Tracheal diameter, course, nodule/mass Bronchiectasis
Pleura/diaphragm	Costal/diaphragmatic/fissural pleural surfaces Diaphragmatic contour/position

1.3 Technical Quality (Table 1.2)

The initial evaluation of any chest radiograph should include a determination of the technical adequacy of the examination to confirm that it is of adequate quality for interpretation. This step is often overlooked, which can lead to both overdiagnosis (as low lung volume may simulate lung disease) and underdiagnosis (motion or rotation may limit proper evaluation of the lungs, mediastinum, and hila). There are five main factors to be assessed.

On a properly positioned frontal chest radiograph, the spinous processes should align with an imaginary vertical line drawn midway between the clavicular heads. The dorsal wrists should be placed on the waist with elbows oriented anteriorly to rotate the scapulae laterally so that they are not superimposed on the upper lungs. Radiographic penetration should allow faint visualization of the vertebral bodies and disc spaces through the mediastinum, with the lungs gray in density and the pulmonary vessels easily seen. Motion is detected by noting the sharpness of the superior cortices of the ribs, vessel margins, and diaphragmatic contours. Proper inspiration is assessed by noting the position of the top of the right hemidiaphragm with respect to the ribs; this point should correspond to the sixth anterior rib or tenth posterior rib at the mid-clavicular line. Artifacts including faulty detectors or visible grid lines can be seen in the digital radiography systems used for obtaining virtually all conventional chest radiographs in a modern radiology department [1].

Key Point

- Evaluation of proper chest radiographic technique involves analysis of patient positioning, proper mediastinal penetration, absence of motion, adequate lung volumes, and the detection of artifacts.

Table 1.2 Evaluating the technical adequacy of chest radiographs

Technical parameter	Assessment
Positioning	Rotation, kyphosis/lordosis
Penetration	Visualization of vertebral interspaces
Motion	Sharpness of hemidiaphragms, ribs, vessels
Lung volumes	Position of diaphragm relative to ribs
Artifacts	Detector drops, grid lines

1.4 Support/Monitoring Devices (Tubes/Lines/Catheters/Pacemakers) (Table 1.3) [2]

Chest radiographs, particularly those obtained in a critical care setting, can demonstrate a broad array of different tubes, vascular catheters, cardiac pacemakers/defibrillators, and other monitoring or therapeutic devices. While in the hospital setting, chest radiographs are typically obtained to confirm proper positioning and to exclude complications following placement of a tube or line; the recognition of one or more of these devices can provide important clues to underlying disease entities.

1.5 Chest Wall

The symmetry of normal chest wall structures such as the breast shadows in females and the spine, ribs, and shoulders should be analyzed to detect chest wall abnormalities. Poland syndrome is a congenital anomaly in which there is unilateral underdevelopment of the musculature of the chest wall. Nonsurgical absence of a portion of a rib or vertebral body may be instrumental in making the diagnosis of malignancy. Congenital deformities such as pectus excavatum can mimic middle lobe disease, as this chest wall deformity creates a vague opacity overlying the region of the middle lobe on frontal radiography (Fig. 1.1). Rib destruction adjacent to a peripheral lung mass is virtually diagnostic of chest wall involvement by lung cancer. Benign pressure erosion of a rib is characteristic of neurogenic neoplasms or chest wall vascular abnormalities such as dilated intercostal arteries in a patient with coarctation of the aorta. In patients with anasarca

Table 1.3 Common support/monitoring devices on chest radiography




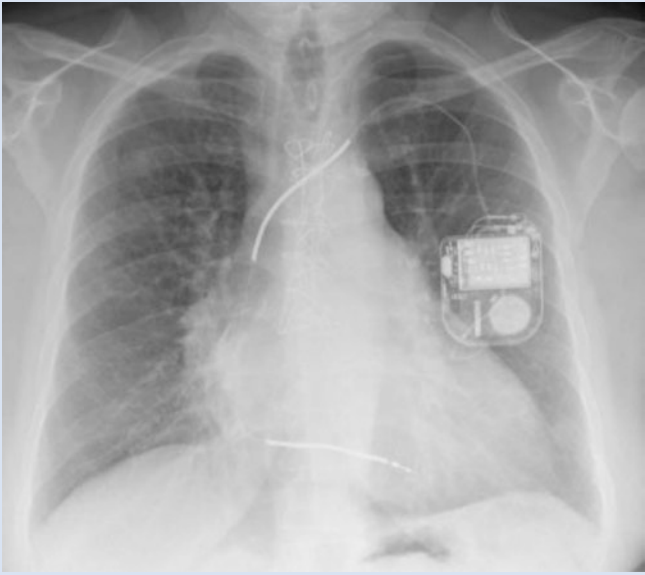
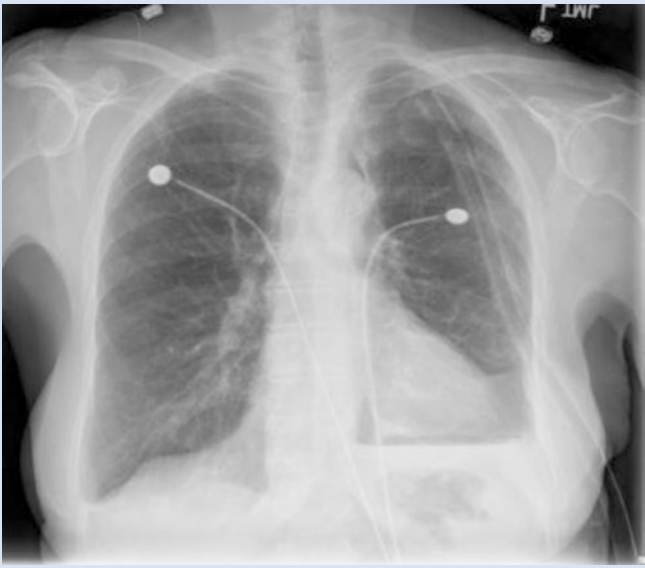
Device	Normal appearance
Endotracheal tube	 A frontal chest radiograph showing an endotracheal tube. The tube is visible as a thin, dark line descending from the top of the image, passing through the trachea, and terminating approximately 2-3 cm above the carina. The lungs are clear, and the heart and mediastinum are within normal limits. There are also some faint lines representing other medical devices or leads.
Nasogastric feeding tube	 A frontal chest radiograph showing a nasogastric feeding tube. The tube is visible as a thin, dark line descending from the top of the image, passing through the nasal cavity, the pharynx, and the esophagus, and curving downwards into the stomach. The lungs are clear, and the heart and mediastinum are within normal limits. There are also some faint lines representing other medical devices or leads.

Table 1.3 (continued)

Device	Normal appearance
Central venous catheters	 A frontal chest radiograph showing a central venous catheter (CVC) in place. The catheter is visible as a thin, dark line originating from the right side of the neck and extending down to the level of the superior vena cava (SVC) junction, just above the heart shadow. The lungs appear clear, and the heart size is within normal limits.
Pacemaker/defibrillator	 A frontal chest radiograph showing a pacemaker or defibrillator device implanted in the left anterior chest wall. The device is a rectangular, metallic-looking box. Two leads are visible: one extending from the device to the right atrium and another extending to the right ventricle. The lungs are clear, and the heart size is normal.
Chest tube	 A frontal chest radiograph showing two chest tubes (thoracostomy tubes) in place. Each tube is visible as a thin, dark line with a circular hub at the insertion site on the chest wall. The tubes are positioned in the pleural spaces on both sides. The lungs appear clear, and there is no evidence of pneumothorax or significant pleural effusion.

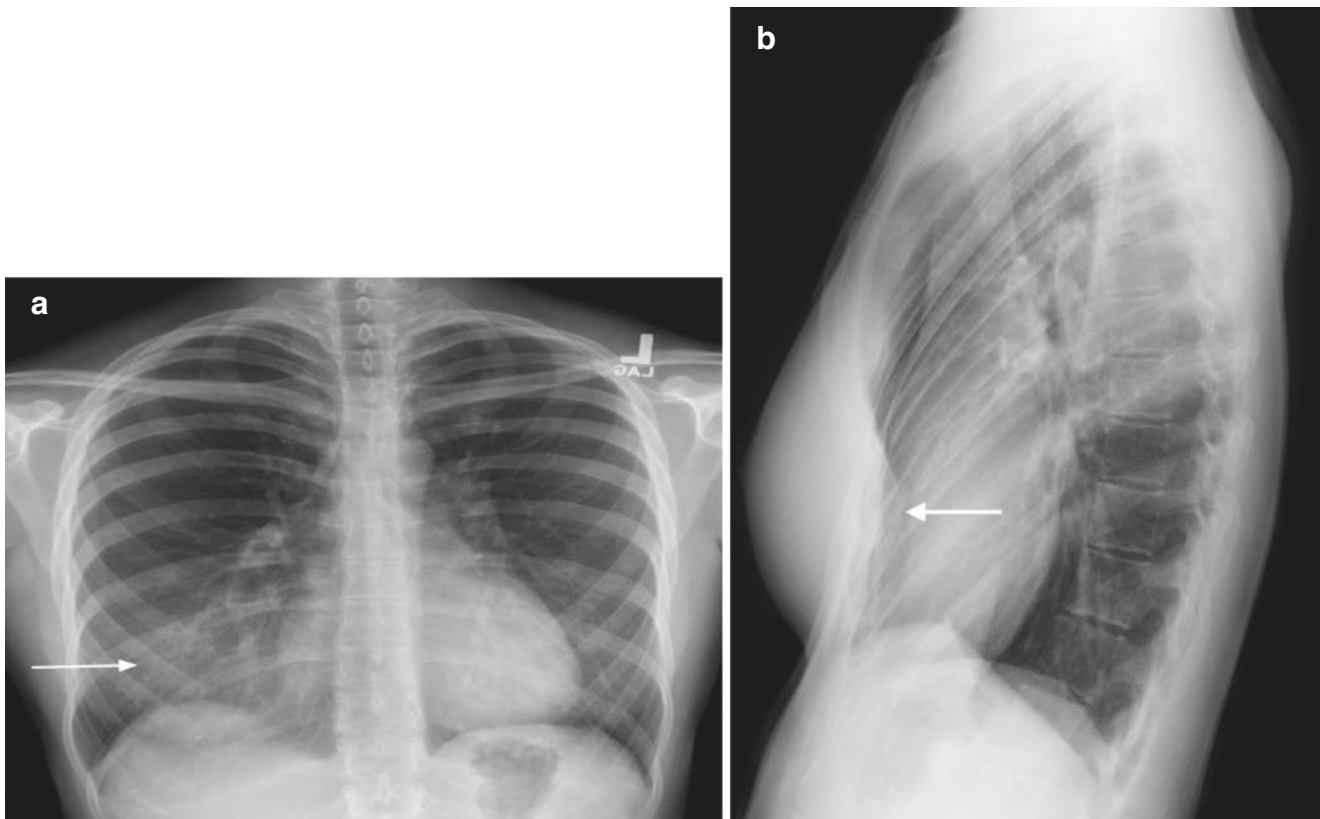


Fig. 1.1 (a, b) Pectus excavatum chest wall deformity mimicking middle lobe disease. (a) Frontal chest radiograph of a 25-year-old female demonstrates a vague opacity overlying the medial right lower lung

(arrow). (b) Lateral radiography shows the characteristic posterior deformity of the lower sternum (arrow) representing pectus excavatum

Table 1.4 Chest wall abnormalities

Finding	Condition
Absence	S/P mastectomy, Poland syndrome
Shape	Pectus excavatum, carinatum
Bone destruction	Peripheral lung cancer, metastasis, infection
Swelling	Anasarca, localized edema
Mass	Breast cancer
Calcification	Dermatomyositis, sarcoma, tumoral calcinosis
Gas	Air leak from chest, S/P laparoscopy, S/P drainage of pneumothorax

due to fluid administration, there may be marked swelling of the soft tissues lateral to the ribs. Larger chest wall masses may produce an “incomplete border sign” radiographically, as the mass creates a visible interface with atmospheric air (or if intrathoracic with the adjacent lung). Soft tissue calcification may indicate prior trauma (myositis ossificans), collagen vascular disease (dermatomyositis), or the presence of a vascular lesion (hemangioma) or a bone-forming malignancy (osteosarcoma or chondrosarcoma) [3]. Gas within the chest wall could indicate an air leak in the setting of trauma, pneumomediastinum, or pneumothorax (Table 1.4).

Key Point

- Chest wall masses typically demonstrate an incomplete border sign as only a portion of the circumference of the mass is typically outlined by atmospheric air or intrapulmonary gas.

1.6 Mediastinum

The mediastinum is the space between the mediastinal pleural reflections bound anteriorly by the sternum and posteriorly by the thoracic vertebrae. It courses from the thoracic inlet superiorly to the diaphragm inferiorly. It contains the heart, pericardium, central great vessels, esophagus, trachea, carina and proximal main stem bronchi, the thoracic duct, lymph nodes, and mediastinal fat. The radiologist must be familiar with the normal mediastinal structures, their contours, and the normal mediastinal lines, stripes, and interfaces to detect mediastinal abnormalities radiographically [4].

1.6.1 Heart

The right cardiac border is formed by the right atrium. From inferior to superior, the left cardiac border is formed by the left ventricle and a small portion of the left atrial appendage. The right ventricle projects anteriorly and inferiorly on the lateral chest radiograph, with the posterior cardiac border formed by the left ventricle inferiorly and the left atrium superiorly.

The heart must be assessed for its shape, size, and location. Abnormal cardiac shift may reflect ipsilateral loss of volume (e.g., lobar atelectasis) or contralateral increased volume (e.g., a large pneumothorax). The normal pericardium is not visible radiographically. Enlargement of the cardiac silhouette may result from cardiac enlargement and/or pericardial effusion. When large, the latter may manifest with a “water bottle heart” on frontal chest radiographs or with the “epicardial fat pad sign” on lateral radiography. The “epicardial fat pad sign” results from visualization of pericardial effusion as a curvilinear band of soft tissue >2 mm thick outlined by mediastinal fat anteriorly and subepicardial fat posteriorly. Constrictive pericarditis may manifest with linear pericardial calcification. Cardiac calcifications may correspond to coronary artery, valvular or annular calcifications, or curvilinear calcification in a left ventricular aneurysm from prior myocardial infarction.

1.6.2 Systemic Arteries

The normal aortic arch is readily visible on radiography and characteristically produces an indentation on the left tracheal wall. With increasing aortic atherosclerosis and tortuosity, a larger portion of the aorta is visible and may exhibit intimal atherosclerotic calcification. The left para-aortic interface projects through the left heart and courses vertically toward the abdomen. The left subclavian artery is seen as a concave left supra-aortic mediastinal interface on frontal chest radiography. A right aortic arch is usually associated with a right descending thoracic aorta. In the absence of associated congenital heart disease, right aortic arch is usually associated with non-mirror image branching characterized by an aberrant left subclavian artery which may be seen as an indentation on the posterior trachea on lateral chest radiography.

1.6.3 Systemic Veins

The azygos arch is visible at the right tracheobronchial angle and normally measures <1 cm in the upright position. The azygos arch may be contained within an accessory azygos fissure, an anatomic variant. Enlargement of the azygos arch

may occur in azygos continuation of the inferior vena cava, in which the vertical portion of the azygos vein manifests as a right-sided vertical mediastinal interface.

The right lateral margin of the superior vena cava is normally visible as it interfaces with the medial right upper lobe. The inferior vena cava may be visible as it creates a concave interface with the right lower lobe in the right cardiophrenic angle prior to its entry into the right atrium. The posterior margin of the inferior vena cava is most evident on lateral radiography as its posterior concave margin is outlined by lung.

1.6.4 Pulmonary Arteries

Enlargement of the central pulmonary arteries may represent pulmonary hypertension and is typically associated with enlargement of the pulmonary trunk. The pulmonary trunk is visible as a left mediastinal interface located above the heart and below the aorta on frontal chest radiography.

1.6.5 Lines, Stripes, and Interfaces [5]

The anterior and posterior junction lines represent the interface between the right and left upper lobes anterior to the great vessels (anterior junction line) (Fig. 1.2) and posterior to the esophagus, superior to the aortic arch, and anterior to the upper thoracic spine (posterior junction line). These lines may be thickened by fat, lymphadenopathy, or mediastinal masses. The paravertebral stripes may be thickened by lymphadenopathy fat or may be displaced laterally by a paravertebral hematoma or infection. An abnormal convex contour of the upper azygoesophageal recess may result from subcarinal lymphadenopathy or a bronchogenic cyst, while a hiatus hernia often produces convexity of the lower 1/3rd of the azygoesophageal recess. Convexity of the aortopulmonary reflection normally a flat or concave interface below the aortic arch and above the main pulmonary artery may be caused by lymphadenopathy in the aortopulmonary window, mediastinal mass, or anomalous vasculature.

1.6.6 Mediastinal Masses (Table 1.5) [6]

Mediastinal masses include primary and secondary neoplasms, mediastinal cysts, vascular lesions, glandular enlargement (thyroid and thymus), and hernias (hiatus and Morgagni). As 10% of mediastinal masses are vascular in etiology, a vascular lesion should always be considered in a patient with a mediastinal contour abnormality.

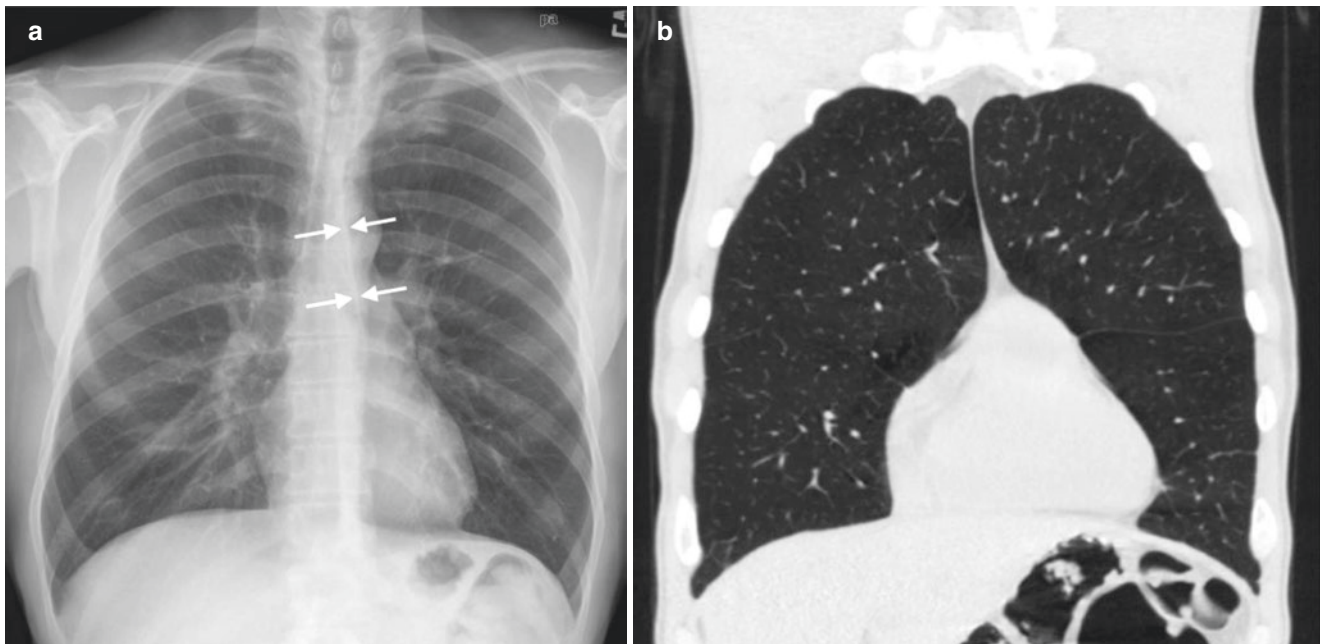


Fig. 1.2 Anterior junction line on frontal chest radiograph with CT correlation (a,b). (a) Frontal chest radiograph shows an obliquely oriented linear opacity (arrows) overlying the upper mediastinum. (b) Coronal multi-detector CT scan at lung windows through the anterior

chest shows that the anterior junction line represents the right and left upper lobes (and corresponding pleural layers) that contact one another anterior to the mediastinum

Table 1.5 Differential diagnosis of mediastinal masses

Anterior	Middle	Posterior
Lymphoma	Lung cancer	Schwannoma/ neurofibroma
Thymic neoplasm	Lymph node enlargement/mass	Ganglion cell tumor
Germ cell neoplasm	Foregut/pericardial cyst	Descending aortic aneurysm
Thyroid goiter	Hiatus hernia	Paravertebral hematoma/abscess

The first step in the assessment of a mediastinal mass is determining that there is indeed a mediastinal abnormality. Focal unilateral mediastinal masses are typically primary neoplasms, enlarged lymph nodes, cysts, and vascular aneurysms or anomalous vessels. While diffuse symmetric mediastinal widening without mass effect can be seen in mediastinal lipomatosis, when lobulated or asymmetric, it should suggest lymphadenopathy in advanced lung cancer, metastatic disease, or lymphoma (Fig. 1.3) or in patients with chest trauma mediastinal hematoma associated with vascular injury. Mediastinal masses should then be localized within a mediastinal compartment based on the lateral chest radiograph. For the purposes of localizing masses and providing a concise differential diagnosis, the mediastinum is divided radiographically into the anterior, middle, and posterior compartments [6]. The middle mediastinum encompasses the heart, pericardium, aorta and great

vessels, systemic and pulmonary veins, trachea, carina, and esophagus. Ancillary findings should be noted such as benign pressure erosion in patients with paravertebral masses (typical of neurogenic tumors). The cervicothoracic sign or obscuration of an abnormal mediastinal contour as it extends above the clavicle into the neck allows lesion localization in both the thorax and the neck, for which the most frequent etiology is intrathoracic goiter. Clinical factors such as age, gender, and presence or absence of symptoms allow the radiologist to provide a focused differential diagnosis prior to proceeding to cross-sectional imaging. Mediastinal widening in the setting of trauma may represent hemorrhage from traumatic vascular injury.

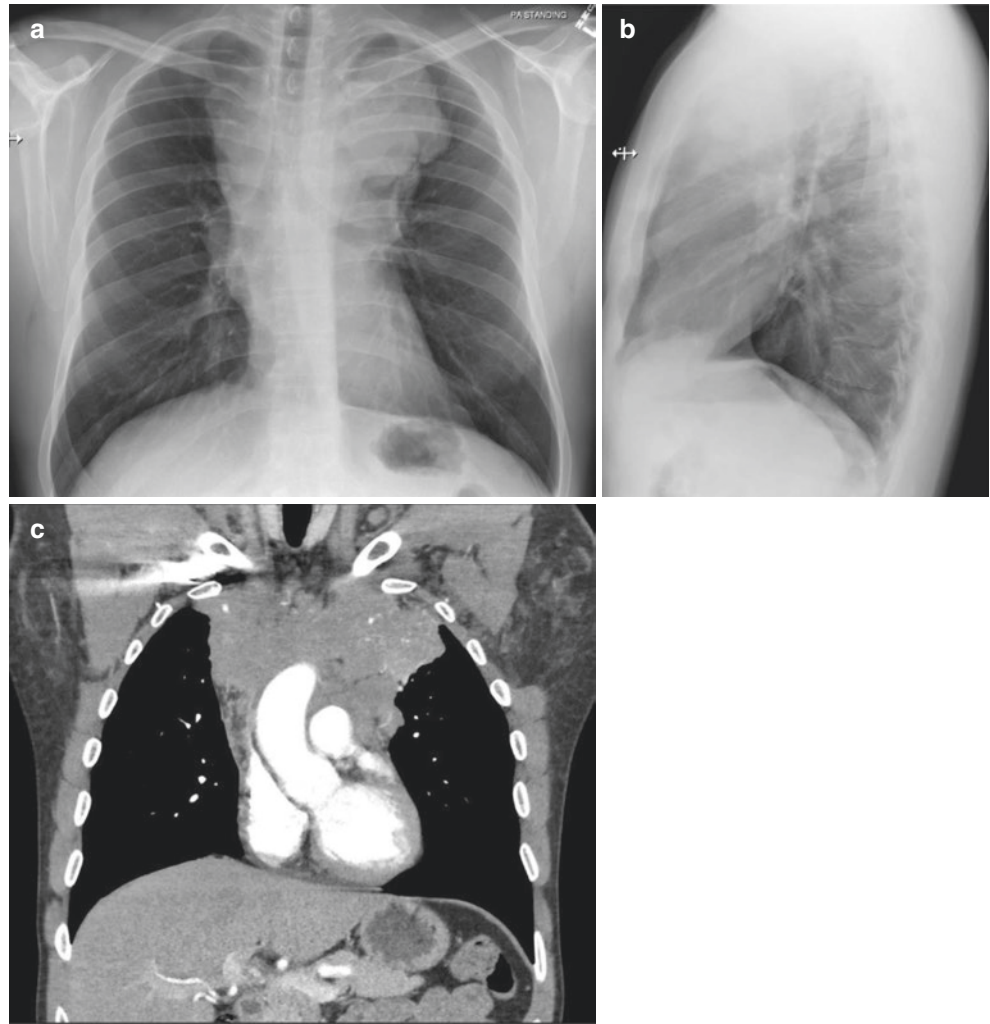
Key Point

- The most common anterior mediastinal masses in adults are lymphoma and thymic neoplasms.

1.6.7 Mediastinal Calcification

The most common cause of mediastinal/hilar calcifications is calcified lymph nodes from prior granulomatous disease such as tuberculosis, histoplasmosis, and sarcoidosis. Patients with treated mediastinal lymphoma may

Fig. 1.3 Anterior mediastinal mass due to Hodgkin lymphoma (a-c). (a,b) Frontal (a) and lateral (b) chest radiographs of a 37-year-old man with cough and weight loss show a large lobulated mass mediastinum. (c) Coronal contrast-enhanced CT through the anterior chest shows a large, locally invasive soft tissue mass subsequently proven to reflect nodular sclerosing Hodgkin lymphoma



demonstrate mass-like calcification, while specific mediastinal neoplasms such as thymoma and mature teratomas may contain de novo calcification evident radiographically.

1.6.8 Pneumomediastinum

While gas may normally be evident radiographically within the trachea, central bronchi, and esophagus, mediastinal gas located outside of these structures is abnormal and usually reflects air leak from the lung or disruption of the central airways or esophagus. Pneumomediastinum is seen as linear and curvilinear lucencies outlining mediastinal structures such as the heart, trachea, and central diaphragm. The most common cause of pneumomediastinum is alveolar rupture in patients with airway obstruction due to asthma or intubated patients receiving mechanical ventilation. Blunt chest trauma can also lead to alveolar

rupture and pneumomediastinum. The combination of pneumomediastinum with left lower lobe lung consolidation and a left pleural effusion or pneumothorax in a patient who has had prolonged vomiting or retching should prompt consideration of esophageal rupture or Boerhaave syndrome, which is a surgical emergency associated with high mortality.

1.7 Hila

On normal frontal chest radiographs, the right hilum is lower than the left in 97% of cases, and the hila are at the same level in 3% of cases [7]. Alterations of this relationship should suggest volume loss on the affected side due to atelectasis, scarring, or prior lung resection. The right hilum is anterior to the left on lateral chest radiography. The intermediate stem line, visible on the lateral chest radiograph, represents the posterior wall of the bronchus intermedius and

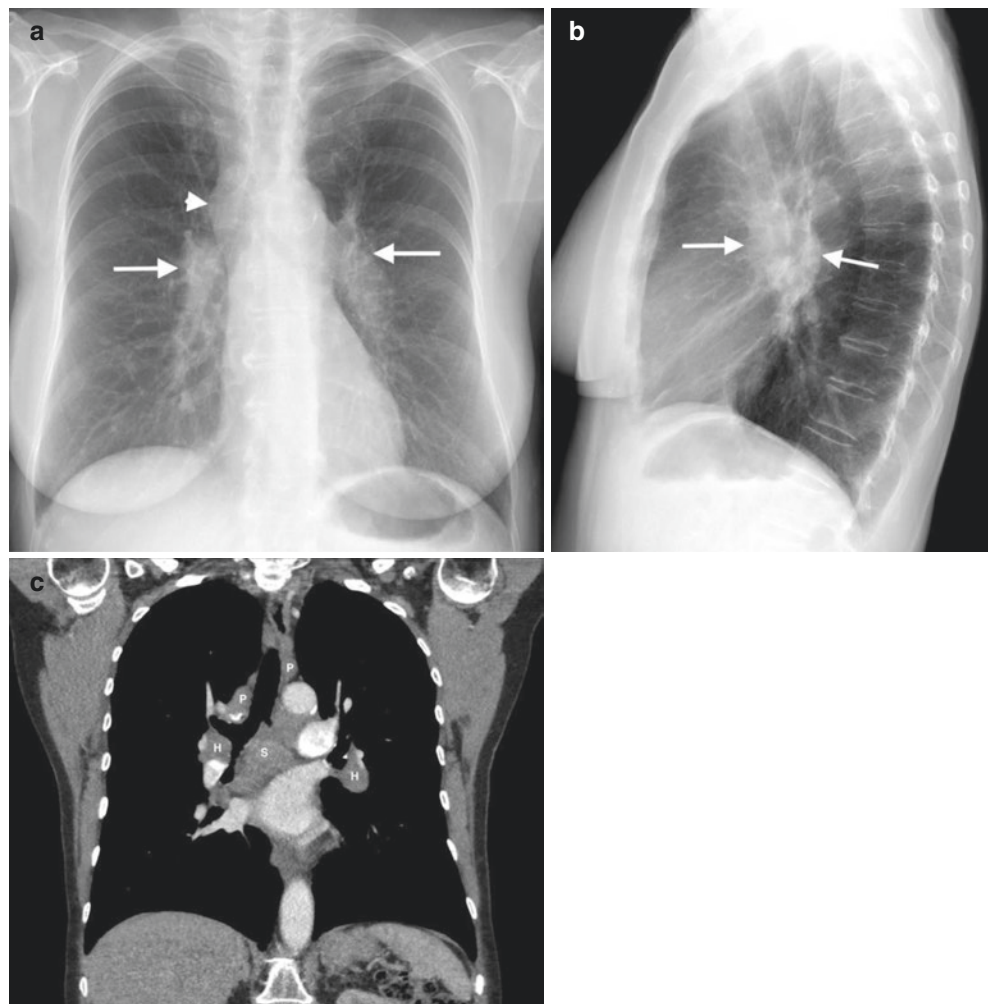
should be assessed for abnormal thickening which may be seen in interstitial edema and central malignancies.

Hilar disease may manifest radiographically as increase (Table 1.6) or decrease in size, an increase in density, or abnormal convexity of the hilum or hila. Hilar enlargement most often results from a central neoplasm, lymph node enlargement (Fig. 1.4), or enlarged central pulmonary arteries as in pulmonary hypertension. The *hilar convergence sign* refers to enlarged vessels coursing toward the enlarged hilum and signifies a vascular etiology.

Table 1.6 Causes of hilar enlargement

Unilateral	Bilateral
Lung cancer	Sarcoidosis
Infection (granulomatous)	Metastatic lymph node enlargement
Metastatic lymph node enlargement	Pulmonary arterial hypertension
Lymphoma	Lymphoma
Valvular pulmonic stenosis (left)	Infection (granulomatous)

Fig. 1.4 (a–c) Sarcoidosis manifesting as bilateral hilar and mediastinal lymph node enlargement. (a) Frontal chest radiograph of a 71-year-old woman with nonproductive cough shows bilateral hilar (arrows) and right paratracheal (arrowheads) lymph node enlargement. (b) Lateral radiograph confirms enlargement and increased density of the bilateral hila as well as soft tissue in the inferior hilar window (the so-called doughnut sign) consistent with bilateral hilar and mediastinal lymphadenopathy (arrows). (c) Contrast-enhanced coronal MIP at mediastinal windows at the level of the carina confirms enlarged hilar (H), bilateral paratracheal (P), and subcarinal (S) lymph nodes



1.8 Lungs

1.8.1 Lung Volumes

Lung volume may be increased in obstructive diseases such as emphysema and is reduced in restrictive diseases such as pulmonary fibrosis and in patients with pleural fibrosis (“trapped lung”), neuromuscular disease (myasthenia gravis, amyotrophic lateral sclerosis, diaphragmatic dysfunction in systemic lupus erythematosus), or extrathoracic disorders (obesity, ascites).

Atelectasis may involve the entire lung, a lobe (Fig. 1.5), and a pulmonary segment [8] or may be subsegmental. Obstructive (resorption) atelectasis is characterized by absence of intrinsic air bronchograms. It may result from endoluminal obstruction, most often from a mucus plug as seen in asthma, bronchitis, or mechanically ventilated patients, although a centrally obstructing neoplasm such as lung cancer must be excluded.

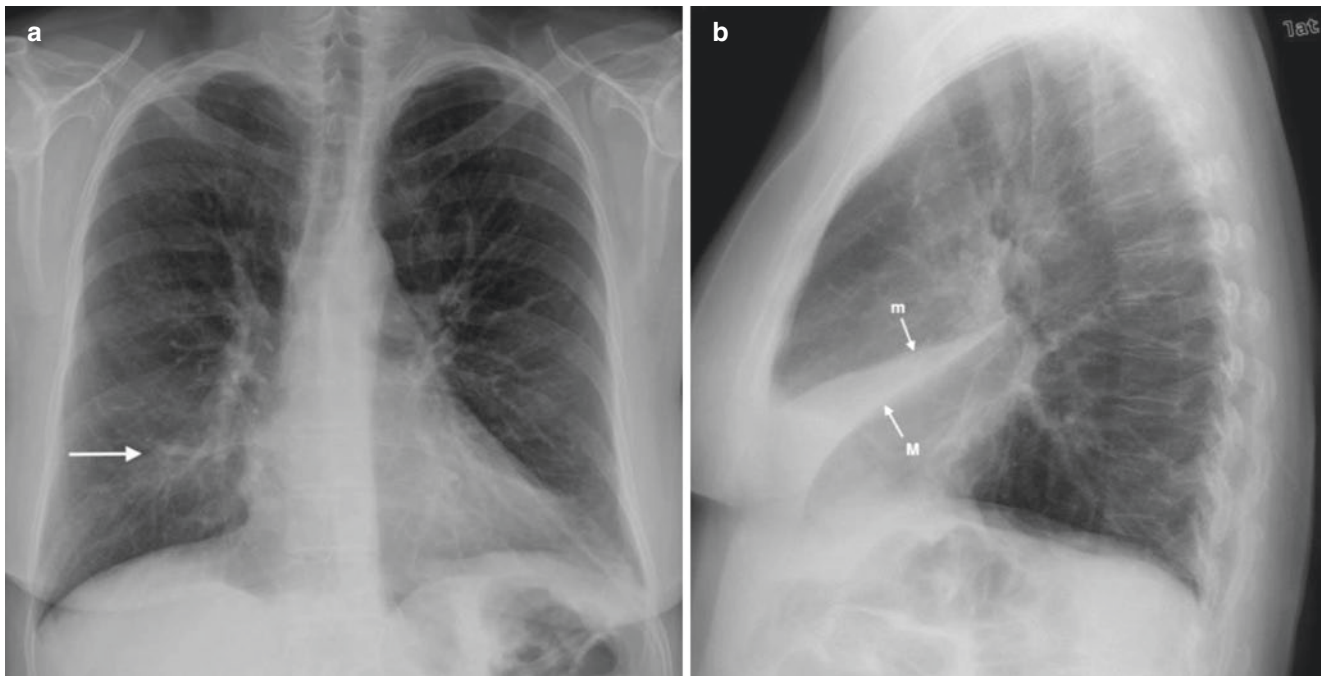


Fig. 1.5 Middle lobe atelectasis (a,b). (a) Frontal radiograph shows a vague opacity (arrow) overlying the lower medial right lung partly obscuring the right heart border. (b) The lateral radiograph shows an atelectatic middle lobe outlined by displaced minor (m) and major (M) fissures

Relaxation (passive) atelectasis often results from mass effect upon the lung, most commonly pleural effusion. Cicatricial atelectasis is due to pulmonary fibrosis. Rounded atelectasis occurs adjacent to pleural thickening in which the subpleural lung, most commonly in the lower posterior part of the chest, “folds” upon itself.

Direct signs of lobar atelectasis include fissural displacement (Fig. 1.5), bronchovascular crowding, and shift of a preexisting lung nodule or calcified granuloma. Indirect signs include increased pulmonary density, ipsilateral mediastinal shift, hilar displacement, ipsilateral hemidiaphragm elevation, and compensatory hyperinflation of the adjacent lung.

Key Point

- The most concerning cause of obstructive (resorptive) atelectasis in an adult is an endobronchial neoplasm such as lung cancer or a carcinoid tumor.

1.8.2 Parenchymal Opacities

Parenchymal opacities include air space and interstitial processes. Pneumonia typically manifests with air space opacification due to alveolar filling by purulent material and may be lobar or sublobar (Fig. 1.6) or may manifest with patchy pulmonary opacities. Air space opacification often exhibits

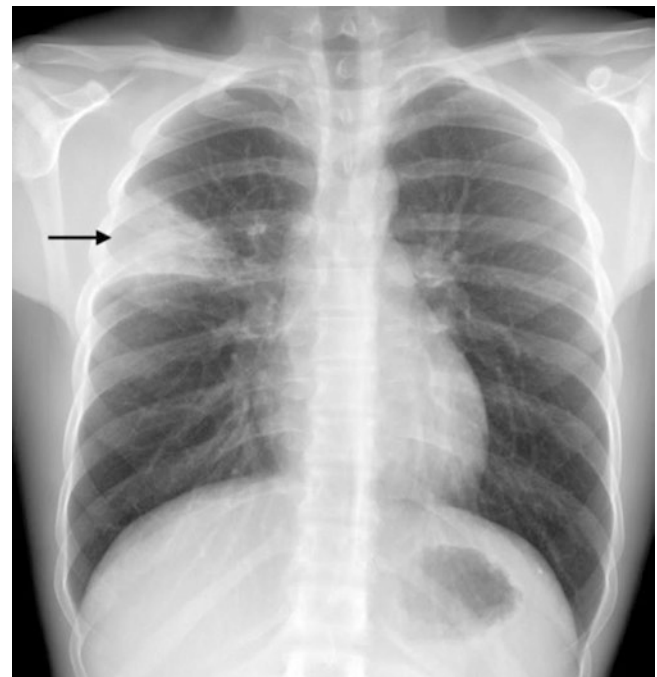


Fig. 1.6 Subsegmental right upper lobe pneumonia as air space opacification. Frontal chest radiograph of a 17-year-old with cough and fever shows a focal area of subsegmental right upper lobe air space opacification (arrow) reflecting pneumonia

intrinsic air bronchograms and may also result from alveolar edema or hemorrhage (Table 1.7).

Interstitial opacities may manifest with reticular, linear, and/or small nodular opacities. As the normal interstitium is

not visible radiographically, visualization of peripheral subpleural reticular opacities is always abnormal. A reticulonodular pattern occurs when abnormal reticular opacities are superimposed on micronodular opacities. Interstitial opacities frequently result from interstitial edema characterized by perihilar haze, peribronchial thickening, septal thickening (Kerley B lines), and subpleural edema often associated with cardiomegaly and pleural effusion. Associated radiographic findings can help limit the differential diagnosis of interstitial disease (Table 1.8).

Cells and fibrosis may also infiltrate the pulmonary interstitium, producing reticular and reticulonodular interstitial opacities in diseases such as sarcoidosis, silicosis, and lymphangitic carcinomatosis.

The idiopathic interstitial pneumonias are a distinct group of disorders often characterized by basilar predominant pulmonary fibrosis associated with volume loss [9]. The diagnosis usually requires further imaging with high-resolution chest CT (HRCT) (Fig. 1.7).

Table 1.7 Differential diagnosis of air space opacification (ASO)

Finding(s)	Disease
Focal/segmental	Pneumonia, contusion, infarct, lung cancer (adenocarcinoma)
Lobar	Pneumonia, endogenous lipoid pneumonia, adenocarcinoma
Patchy	Pneumonia, aspiration, organizing pneumonia, contusions adenocarcinoma, metastases
Diffuse	Edema, hemorrhage, pneumonia
Perihilar	Edema, hemorrhage
Peripheral	Eosinophilic pneumonia, organizing pneumonia, acute respiratory distress syndrome, contusions
Rapidly changing/resolving	Edema, eosinophilic pneumonia, hemorrhage

Table 1.8 Ancillary findings in patients with ILD and differential considerations

Finding(s)	Disease
Hilar lymph node enlargement	Sarcoidosis, lymphangitic carcinomatosis, viral pneumonia
Clavicular/osseous erosions	Rheumatoid arthritis associated UIP
Pleural effusions	Infection, edema
Pleural plaques	Asbestosis
Hyperinflation	Langerhans cell histiocytosis, stage IV sarcoidosis, lymphangioleiomyomatosis, emphysema with UIP
Esophageal dilatation	Scleroderma associated UIP, recurrent aspiration
Conglomerate masses	Silicosis/coal worker's pneumoconiosis, sarcoidosis, talcosis
Basilar sparing	Langerhans cell histiocytosis, sarcoidosis
Basilar predominance	UIP, fibrotic NSIP, aspiration

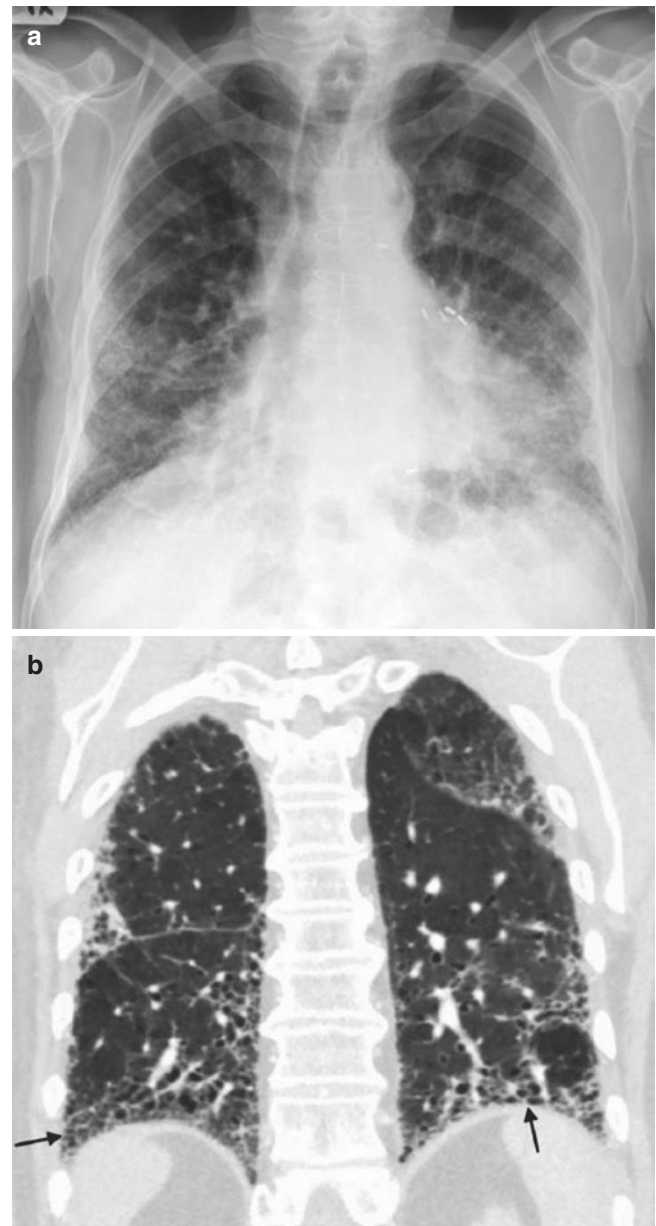
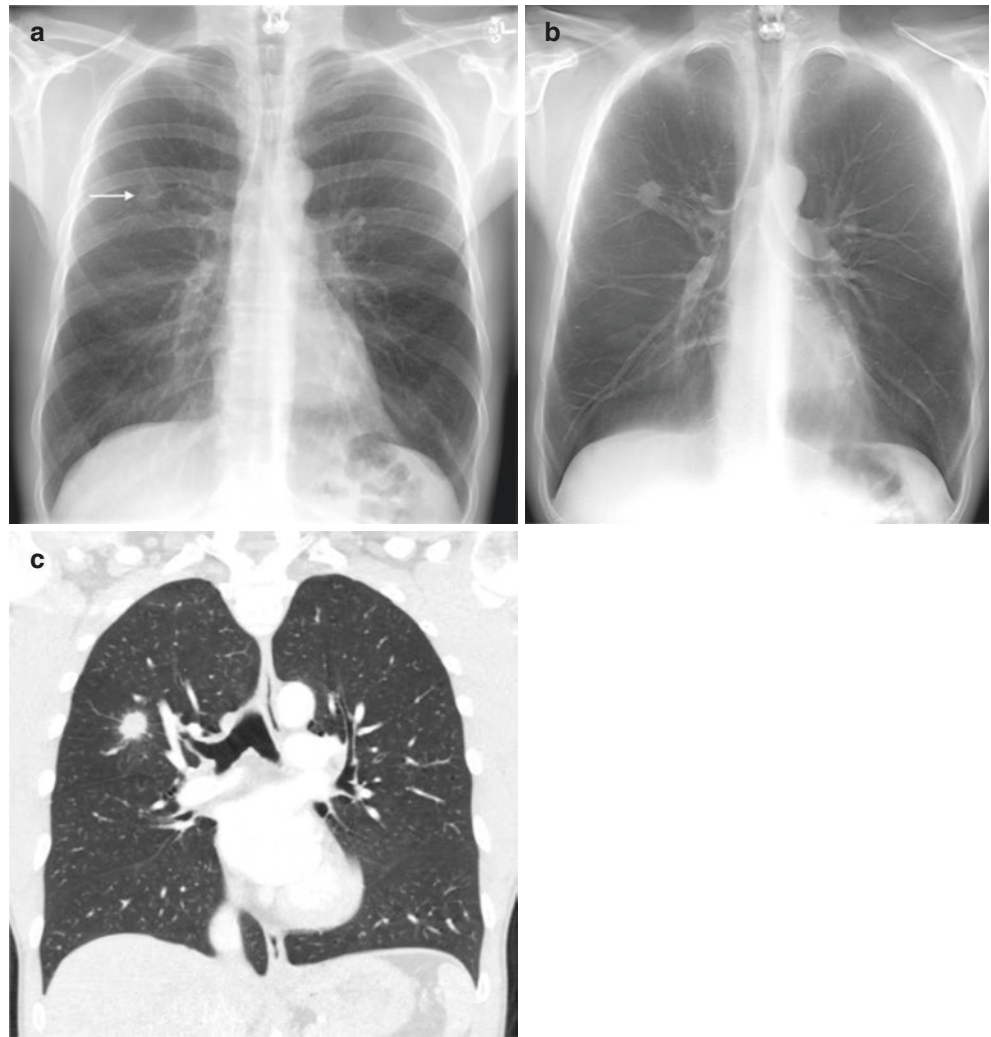


Fig. 1.7 Usual interstitial pneumonia (UIP)/idiopathic pulmonary fibrosis (IPF) as coarse basilar reticular ILD (a,b). (a) Frontal chest radiograph of an 84-year-old man with progressive shortness of breath demonstrates basal predominant coarse reticular opacities. (b) Coronal CT through the posterior chest at lung windows shows lower lobe subpleural reticulation with honeycombing (arrows) diagnostic of a UIP pattern

Key Point

- Chronic, basal predominant ILD is most often due to usual interstitial pneumonia (UIP) or fibrotic nonspecific interstitial pneumonia (NSIP). Both conditions produce basilar reticular interstitial opacities with fibrosis and can be difficult to distinguish clinically and on imaging; biopsy is often necessary for definitive diagnosis in patients lacking CT findings of UIP.

Fig. 1.8 Solitary pulmonary nodule with spiculation (a–c). (a) Frontal chest radiograph of a 43-year-old asymptomatic smoker shows a right upper lobe nodule (arrow) (b,c). Frontal digital tomographic image through the nodule (b) shows a spiculated margin, confirmed on coronal CT at lung windows through the nodule (c). Diagnosis was lung adenocarcinoma



A solitary pulmonary nodule (SPN) is defined as a round or ovoid opacity <3 cm in diameter. A benign pattern of intrinsic calcification in a smooth or slightly lobulated SPN reflects a granuloma or hamartoma and precludes further imaging evaluation [10].

However, the presence of calcification can be difficult to discern on standard high-kVp chest radiographs. CT provides superior contrast resolution, and thin-section scans can detect calcification that is not evident radiographically. The majority of SPNs are indeterminate on radiography and require further assessment and characterization with thin-section computed tomography (CT) to exclude malignancy (Fig. 1.8)(Table 1.9).

Key Point

- While chest radiography can detect a solitary pulmonary nodule (SPN), thin-section CT will almost invariably be needed to characterize an SPN for possible malignancy.

Table 1.9 Common causes of a solitary pulmonary nodule

Granuloma
Hamartoma
Malignancy: lung cancer, carcinoid tumor, metastasis
Focal organizing pneumonia

A pulmonary mass is a round or ovoid pulmonary opacity ≥ 3 cm in diameter and is highly suspicious for malignancy, typically lung cancer. The radiologist should look for pertinent ancillary findings of malignancy including other lung nodules, local invasion of adjacent structures, lymphadenopathy, and pleural effusion.

Abnormal lucency can be difficult to detect radiographically as the lungs are predominantly air filled. The most common localized lucent lesion is a bulla, seen as a focal lucency >1 cm diameter demarcated from adjacent lung by a uniform, thin (<1 mm) wall [11]. Unilateral lucency can relate to technical issues, chest wall defects, or parenchymal abnormalities as seen in the Swyer-James or unilateral hyperlucent lung syndrome, which is a post-infectious obliterative bronchiolitis

that results in air trapping and decreased lung vascularity. Bilateral hyperlucency is most often seen in severe emphysema or in patients with acute asthma exacerbation.

1.9 Airways

The trachea and bronchi should be assessed for size, patency, and course. Tracheal narrowing may be focal or diffuse (Table 1.10) [12]. Focal tracheal narrowing or stenosis most often occurs secondary to mucosal or cartilaginous damage from prolonged intubation. More diffuse tracheal narrowing is most common in patients with COPD in which there is narrowing of the transverse diameter of the tracheal lumen, the so-called saber-sheath trachea. Primary or metastatic airway neoplasms may manifest as endoluminal soft tissue nodules that may be associated with volume loss. Endotracheal tumors may grow to obstruct up to 75% of the airway lumen before symptoms ensue (Fig. 1.9). Airway neoplasms may also manifest as focal or diffuse airway stenosis and must be differentiated from inflammatory conditions. Tracheal dilatation seen in the Mounier-Kuhn syndrome is a rare congeni-

tal condition characterized by tracheal and bronchial dilatation due to atrophy of the muscular and elastic tissues of the trachea and main bronchi. The trachea may deviate toward a region of upper lobe volume loss, as seen in upper lobe fibrosis, or may be displaced by a mass in the thoracic inlet such as an enlarged thyroid.

Bronchiectasis is abnormal irreversible bronchial dilatation and may result from infection, cystic fibrosis, primary ciliary dyskinesia, or allergic bronchopulmonary fungal disease. It is seen radiographically as tram tracks which represent the thickened bronchial walls in cylindrical bronchiectasis and clustered, thin-walled cystic lesions in cystic bronchiectasis.

1.10 Pleura/Diaphragm

Pleural abnormalities manifest radiographically as gas (pneumothorax) or fluid (pleural effusion) in the pleural space or as abnormalities of the pleural surfaces including thickening (pleural plaques, neoplasms) and calcification (pleural plaques, fibrothorax) [13].

Fig. 1.9 Tracheal mass reflecting local invasion by esophageal carcinoma (a–c). (a) Frontal chest radiograph shows lobular contours of the upper mediastinum and thickening of the bilateral paratracheal stripes (arrows). (b) The lateral chest radiograph demonstrates thickening of the anterior and posterior tracheal walls and smooth stenosis of the upper trachea (arrows). (c) Axial contrast CT through the upper chest at mediastinal windows shows a lobulated soft tissue mass involving the anterior wall of the esophagus with invasion of the mediastinum and posterior trachea with marked narrowing of the tracheal lumen

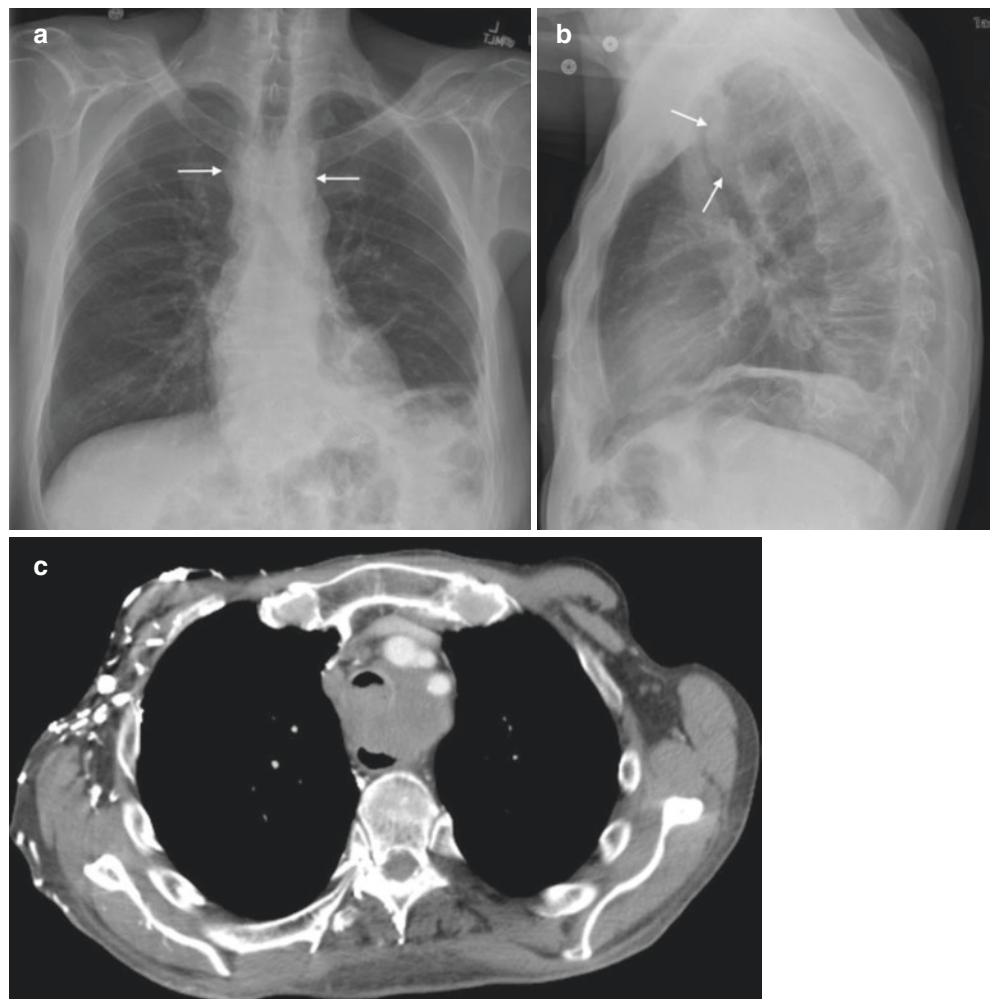


Table 1.10 Tracheal abnormalities seen radiographically

Tracheal deviation	Ipsilateral	Upper lobe volume loss (fibrosis)
	Contralateral	Thyroid/thoracic inlet mass
Tracheal narrowing	Focal	Stenosis post intubation, tracheostomy
		TB, fungal infection
		Thyroid mass (extrinsic)
		Saber-sheath trachea
	Diffuse	Relapsing polychondritis
		Granulomatosis with polyangiitis
Tracheal dilation	Focal	Tracheomalacia
	Diffuse	Pulmonary fibrosis
Tracheal mass		Mounier-Kuhn syndrome (tracheobronchomegaly)
		Squamous cell carcinoma
		Metastasis
		Adenoid cystic carcinoma
		Hamartoma
		Foreign body/mucus

Pneumothorax is seen on upright chest radiography as a superior lucency that parallels the chest wall and outlines the curvilinear visceral pleural line that is inwardly displaced from the chest wall. Pneumothorax may be spontaneous or traumatic. Spontaneous pneumothorax is categorized as primary (no underlying lung disease) and secondary (underlying lung disease).

The radiographic appearance of pleural effusion depends on the amount of fluid, whether the fluid is free-flowing or loculated, and the position of the patient when the radiograph is obtained. A small, free-flowing pleural effusion in an upright patient manifests radiographically as a meniscus blunting the posterior costophrenic sulcus on lateral radiography, with larger effusions blunting the lateral costophrenic sulcus on frontal radiography and effusions exceeding 500 mL in volume obscuring the hemidiaphragm. Loculated pleural effusions are typically infected (so-called parapneumonic effusions and empyemas) and produce biconvex mass-like opacities along the dependent costal pleural surfaces (Fig. 1.10). In such cases, an air fluid level in

Fig. 1.10 Empyema as a loculated pleural effusion (a–c). (a,b) Frontal chest radiograph of a 37-year-old woman with a history of intravenous drug use who presented with fevers and chest pain shows a loculated left basilar and lateral (a) and posterior (b) pleural collection (black arrows), confirmed on contrast-enhanced sagittal CT (c) (white arrows)

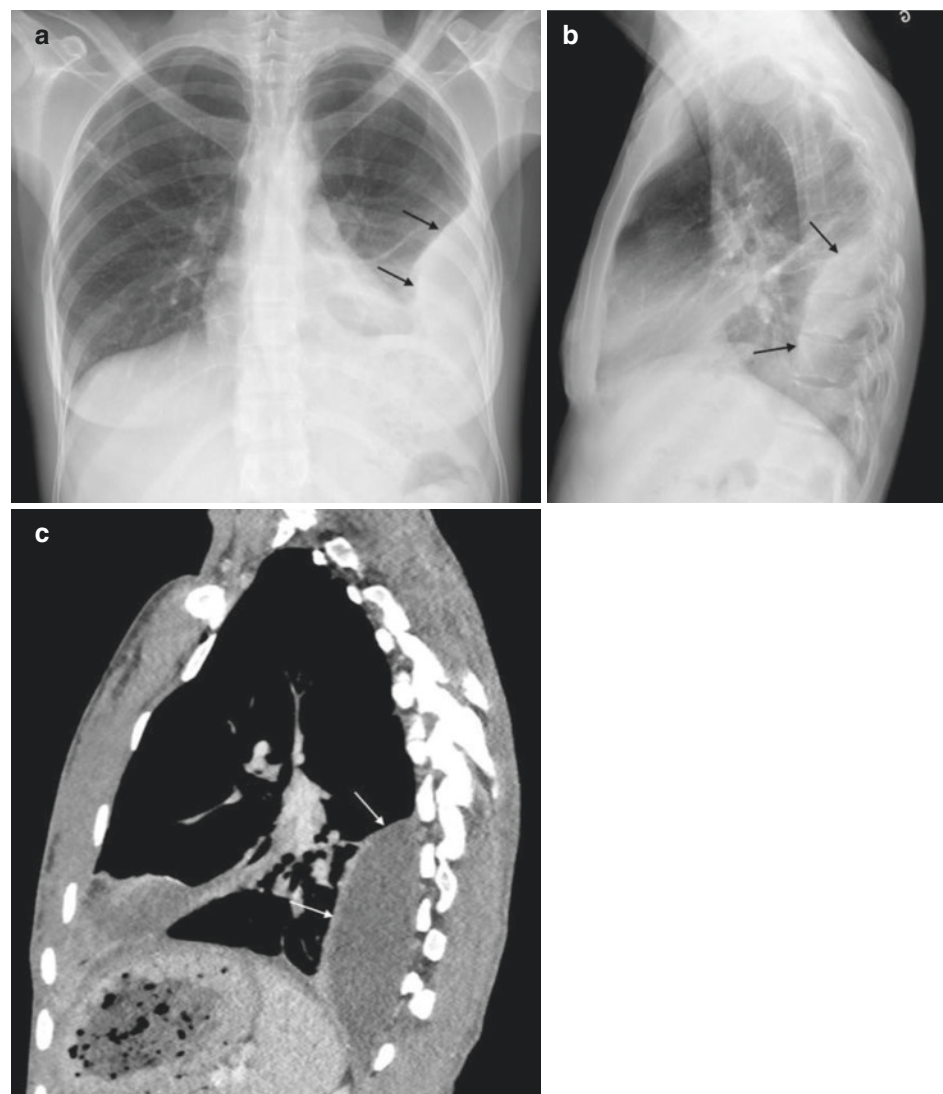
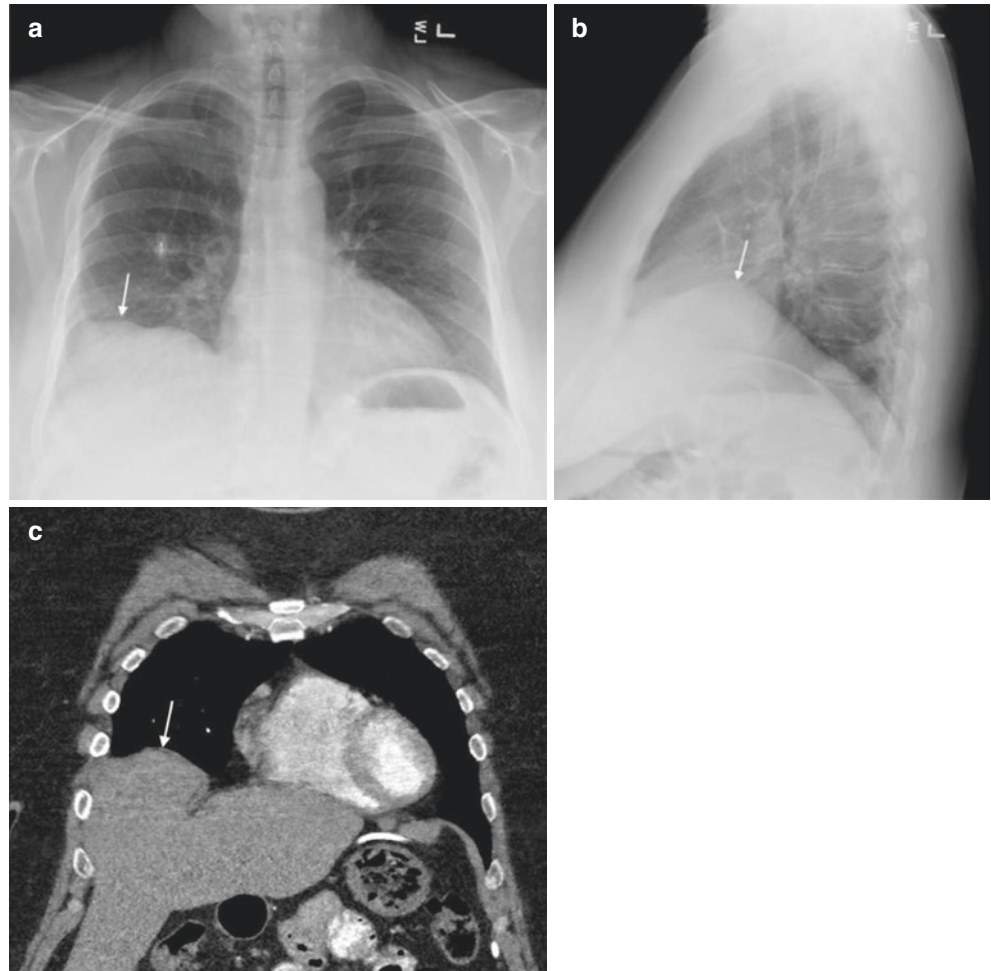


Fig. 1.11 Diaphragmatic eventration (a-c). (a) Frontal and lateral (b) chest radiographs show a focal bulge in the lateral (arrow in (a)) and anterior (arrow in (b)) right hemidiaphragm. (c) Coronal contrast-enhanced CT through the anterior chest at mediastinal windows show the liver projecting into the lower right chest due to eventration of the lateral right hemidiaphragm (arrow)



the pleural space in the absence of prior intervention is diagnostic of a bronchopleural fistula. Massive pleural effusions and pleural effusions with associated pleural nodules should suggest malignancy in the absence of trauma. Identification of circumferential nodular pleural thickening is virtually diagnostic of malignancy, with the main diagnostic considerations including metastatic disease, malignant pleural mesothelioma, and lymphoma.

The diaphragm is a domed structure, with the right slightly higher than the left owing to the position of the heart on the left. A uniformly elevated diaphragm is most often due to weakness or paralysis of the diaphragm, while focal bulges in the diaphragmatic contour are typically due to eventration (thinning) of the diaphragm (Fig. 1.11) or diaphragmatic hernia through a congenital or acquired diaphragmatic defect [14].

Key Point

- Loculated pleural effusions often manifest radiographically as vertically oriented biconvex pleural opacities and are usually associated with underlying lung infection (termed parapneumonic effusions).

1.11 Concluding Remarks

Although considered relatively “low tech” in the age of multi-detector CT, MR, and ultrasound, conventional chest radiography remains an important imaging study in the evaluation of patients with chest symptoms, in assessing hospitalized patients who have tubes or catheters placed for monitoring or treatment, and in screening the chest for asymptomatic disease. Each study should first be evaluated for technical adequacy, followed by a consistent, systematic review of the normal anatomy and structures to allow detection of abnormalities or exclude the presence of disease. Each component of the chest radiograph should be reviewed with findings reported in the same, consistent fashion, ideally in a systematic way that provides the referring clinician with a structured report that parallels the radiographic analysis. While many chest radiographic findings are nonspecific, there are important conditions evident radiographically such as pneumothorax or pneumonia that can direct specific treatment or, as in the case of a non-calcified SPN, allow the radiologist to make recommendations of appropriate imaging follow-up or management.

Take-Home Messages

- An analysis of the technical adequacy of a chest radiographic study is necessary prior to interpretation.
- In critically ill hospitalized patients, chest radiographs performed for the assessment of monitoring or support devices provide important information regarding proper device positioning and help detect complications of placement.
- The radiographic detection of mediastinal abnormalities requires a detailed knowledge of normal mediastinal imaging anatomy and interfaces.
- Lung radiographic abnormalities can be divided into air space and interstitial diseases, solitary pulmonary nodules or masses, and abnormal decreases in density that can be localized, unilateral, or diffuse.
- Diaphragmatic contour abnormalities may be localized, such as in patients with eventration or hernia, or diffuse as in diaphragmatic weakness of paralysis.

References

1. Walz-Flannigan AI, Brossoit KJ, Magnuson DJ, Schueler BA. Pictorial review of digital radiography artifacts. *Radiographics*. 2018;38(3):833–46.
2. Godoy MCB, Leitman BS, de Groot PM, Vlahos I, Naidich DP. Chest radiography in the ICU: part 2, evaluation of cardiovascular lines and other devices. *Am J Roentgenol*. 2012;198(3):572–81.
3. Nam SJ, Kim S, Lim BJ, et al. Imaging of primary chest wall tumors with radiologic-pathologic correlation. *Radiographics*. 2011;31(3):749–70.
4. Whitten CR, Khan S, Munneke GJ, et al. A diagnostic approach to mediastinal abnormalities. *Radiographics*. 2007;27:657–71.
5. Gibbs JM, Chandrasekhar CA, Ferguson EC. Lines and stripes: where did they go?—from conventional radiography to CT. *Radiographics*. 2007;27:33–48.
6. Carter BW, Benveniste MF, Madan R, et al. ITMIG classification of mediastinal compartments and multidisciplinary approach to mediastinal masses. *Radiographics*. 2017;37(2):413–36.
7. Webb WR. Chapter 3: The Pulmonary Hila. In: Webb WR, Higgins CB, editors. *Thoracic imaging: pulmonary and cardiovascular radiology*. 3rd ed. Philadelphia: Wolters Kluwer; 2017. p. 78–82.
8. Abbott GA. Approach to atelectasis and volume loss. In: Rosado-de-Christenson ML, editor. *Diagnostic imaging—chest*. Salt Lake City: Amirsys; 2012. p. 1–56.
9. Sverzellati N, Lynch DA, Hansell DM, Johkoh T, King TE, Travis WD. American thoracic society–European respiratory society classification of the idiopathic interstitial pneumonias: advances in knowledge since 2002. *Radiographics*. 2015;35(7):1849–71.
10. Hodnett PA, Ko JP. Evaluation and management of indeterminate pulmonary nodules. *Radiol Clin N Am*. 2012;50:895–914.
11. Hansell DM, Bankier AA, MacMahon H, McLoud TC, Müller NL, Remy J. Fleischner society: glossary of terms for thoracic imaging. *Radiology*. 2008;246(3):697–722.
12. Heidinger BH, Occhipinti M, Eisenberg RL, Bankier AA. Imaging of the large airways disorders. *Am J Roentgenol*. 2015;205:41–56.
13. Qureshi NR, Gleeson FV. Imaging of pleural disease. *Clin Chest Med*. 2006;27(2):193–213.
14. Nason LK, Walker CM, McNeeley MF, Burivong W, Fligner CL, Godwin JD. Imaging of the diaphragm: anatomy and function. *Radiographics*. 2012;32(2):E51–70.

Open Access This chapter is licensed under the terms of the Creative Commons Attribution 4.0 International License (<http://creativecommons.org/licenses/by/4.0/>), which permits use, sharing, adaptation, distribution and reproduction in any medium or format, as long as you give appropriate credit to the original author(s) and the source, provide a link to the Creative Commons license and indicate if changes were made.

The images or other third party material in this chapter are included in the chapter's Creative Commons license, unless indicated otherwise in a credit line to the material. If material is not included in the chapter's Creative Commons license and your intended use is not permitted by statutory regulation or exceeds the permitted use, you will need to obtain permission directly from the copyright holder.

